STU
FCHPT

# Influence of the counter-anions on the $[Ni(Him)_6]^{2+}$ complex cation (H*im* = imidazole)

**A. Koščíková, L. Krešáková, J. Černák**

*Department of Inorganic Chemistry, Institute of Chemistry, P. J. Šafárik University in Košice, Moyzesova 11, 041 54 Košice, Slovakia*
*andrea.koscikova@student.upjs.sk*

**Abstract:** Four ionic Ni(II) complexes containing the $[Ni(Him)_6]^{2+}$ (H*im* = imidazole) complex cation were prepared: $[Ni(Him)_6](CO_3)\cdot 5H_2O$ (**1**), $[Ni(Him)_6](ac)_2\cdot H_2O$ (**2**, *ac* = acetate), $[Ni(Him)_6](NO_3)_2$ (**3**), and $[Ni(Him)_6]SiF_6$ (**4**); complexes **2** and **4** are new. The prepared complexes were characterized chemically and spectroscopically. Results of X-ray single crystal studies have shown that all four complexes exhibit ionic crystal structures comprising $[Ni(Him)_6]^{2+}$ complex cations, the respective anion(s), and in case of **1** and **2**, additional solvate water molecules. Ni(II) central atoms in all complexes **1**—**4** are hexa-coordinated by six N-atoms originating from monodentate H*im* ligands. While in **1** and **4** the $NiN_6$ chromophore is quite a regular octahedron with only one independent Ni—N bond, as imposed by local symmetry, in **2** and **3** the octahedra are slightly deformed. On the other hand, significant differences were observed in the orientation of H*im* rings within the respective coordination polyhedra.

**Keywords:** Crystal structure, hexa-coordination, imidazole, nickel(II)

## Introduction

Imidazole (H*im*), which is involved in important biological processes, has become an attractive complexing agent over the years. Due to the two nitrogen atoms of which one can be deprotonated, it is promising in metal ion coordination. It may also be active in building supramolecular structures as the protonated nitrogen atom may act as a hydrogen bond donor. Thus, the presence of different counter-anions, given their different geometrical configurations, results in dissimilar supramolecular structures (Ding, 2009; Song, 2008).

Octahedrally coordinated Ni(II) atom is magnetically active ($S = 1$) and its magnetic properties, especially at low temperatures, are governed by the action of axial zero-field splitting parameter $D$. Additional splitting may be induced by the rhombic term of the zero-field splitting parameter $E$. Recently, it has been shown that experimentally obtained values of $D$ (and $E$) can be correlated with the values $D_{str}$ (and $E_{str}$) derived from geometric parameters of Ni(II) coordination polyhedron (Ivaniková, 2006; Mašlejová, 2006; Titiš, 2010; Singh, 2014; Manson, 2020). It is known that small variations in the ligand's composition, alternation of the bridging unit or arrangement of the second coordination sphere including solvating species in the solid state significantly affect magnetic properties of the studied complexes (Juráková, 2022; Brezovan, 2022; Joshi, 2025; Leiszner, 2024). Within our broader interest in Ni(II) complexes (Krešáková, 2021; Šterbinská, 2020; Vráblová, 2016; Černák, 2015), the above information prompted the study of the shape of the homoleptic coordination sphere of selected Ni(II) complex as a function of the counterions quality. As the homoleptic complex, the cation $[Ni(Him)_6]^{2+}$ was chosen due to its easy synthesis and the possibility to crystallize with various counterions. As counterions, two anions with the charge of –1 were chosen, planar nitrate and the more voluminous acetate. Additionally, two counterions with the charge of –2 and different shapes were selected: planar carbonate anion, and the bulkier hexafluoridosilicate anion. As a result of our experiments, four complexes containing $[Ni(Him)_6]^{2+}$ complex cations were prepared, two of which are new. Here, their syntheses, as well as crystal and supramolecular structures are reported. In addition, a detailed comparison of the $NiN_6$ octahedra shape with respect to various counter-anions is provided.

## Material and Methods

### *Chemicals*

$[Ni(ac)_4]\cdot 4H_2O$ (98 %), $[Ni(NO_3)_2]\cdot 6H_2O$ (98 %), $(NH_4)_2SiF_6$ (98 %), imidazole (p. a.), acetonitrile (99.8 %), *n*-butanol (99.8 %), ethanol (96 %), acetone (99.8 %).

### *Synthesis of $[Ni(Him)_6]CO_3\cdot 5H_2O$ (1)*

An acetonitrile-aqueous solution (2:1, 10 ml) of nickel(II) acetate tetrahydrate (0.124 g, 0.5 mmol) was added dropwise to an acetonitrile-aqueous solution (2:1, 10 ml) containing imidazole (0.272 g, 4 mmol) while being stirred (30 min) and heated at 50 °C. The formed dark blue solution was filtered and allowed to stand at room temperature. After

11 days, violet crystals were collected and dried in air. Yield: 38 %.
Anal. [ %], calculated for $C_{19}H_{34}N_{12}O_8Ni$: C 36.97; H 5.55; N 27.23; found: C 37.39; H 5.68; N 27.20.
IR ($cm^{-1}$): 3643s, 3129s, 3014w, 2919w, 2831w, 2715w, 2623s, 1686s, 1543s, 1455s, 1385s, 1323s, 1254s, 1067s, 936s, 908s, 749s, 665s, 619s.

***Synthesis of [Ni(Him)$_6$](ac)$_2$·H$_2$O (2)***
Solid imidazole (0.102 g, 1.5 mmol) was added to the *n*-butanolic solution (10 ml) of nickel(II) acetate tetrahydrate (0.062 g, 0.25 mmol) and stirred for 15 minutes. The resulting blue-green solution was treated solvothermally for 4 h at 130 °C and then slowly cooled to room temperature for 8 hours. From the resulting solution, blue-violet crystals were collected after 2 months. Yield: 59 %.
Anal. [%], calculated for $C_{22}H_{32}N_{12}O_5Ni$: C 43.80; H 5.35; N 27.86; found: C 43.55; H 5.36; N 27.24.
IR ($cm^{-1}$): 3506w, 3129w, 3025w, 2923w, 2834w, 2624w, 1571s, 1537s, 1488s, 1411s, 1322s, 1145s, 1068s, 937s, 904s, 829s, 744s, 665s, 620s.

***Synthesis of [Ni(Him)$_6$](NO$_3$)$_2$ (3)***
Nickel(II) nitrate hexahydrate (0.5 mmol, 0.145 g) and imidazole (3 mmol, 0.204 g) were dissolved in a mixture of acetone (10 ml) and ethanol (10 ml), the obtained blue solution was stirred for 30 minutes. Then, light violet microcrystalline powder of **3** appeared, which was filtered off, washed with 2 ml of ethanol, and dried in air. After four days, violet cubes formed from the blue filtrate. Yield: 29 %.
Anal. [%], calculated for $C_{18}H_{24}N_{14}O_6Ni$: C 36.57; H 4.09; N 33.17; found: C 36.20; H 4.13; N 32.69.
IR ($cm^{-1}$): 3169w, 3137s, 3052w, 2950w, 2859w, 1605w, 1537s, 1489m, 1438m, 1367s, 1323s, 1254s, 1182m, 1138m, 1064s, 935s, 843s, 742s, 665s, 613s.

***Synthesis of [Ni(Him)$_6$]SiF$_6$ (4)***
Reagents nickel(II) nitrate hexahydrate (0.5 mmol, 0.145 g), imidazole (3 mmol, 0.204 g), and diammonium hexafluorosilicate (0.5 mmol, 0.089 g) were dissolved in water (5 ml, 10 ml and 5 ml), mixed, and stirred for 30 minutes. The product in form of purple hexagonal single crystals was collected at room temperature after eight weeks. Yield: 18 %.
Anal. [%], calculated for $C_{18}H_{24}N_{12}F_6SiNi$: C 35.49; H 3.97; N 27.59; found: C 36.21; H 3.95; N 27.17.
IR ($cm^{-1}$): 3288w, 3161m, 3141s, 2945w, 2836w, 1623w, 1532s, 1510m, 1488s, 1432s, 1326s, 1255m, 1176m, 1099s, 1062s, 921m, 865m, 795s, 746s, 693s, 613s.

***Physical measurements***
CHN analyses were performed on a CHNOS Elemental Analyzer vario MICRO instrument (Elementar Analysen systeme GmbH). Infrared spectra were recorded in the range of 4000—400 $cm^{-1}$ on a Nicolet 6700 FT-IR spectrophotometer (Thermo Scientific) using the KBr technique. X-ray powder diffraction patterns were measured on a Ultima IV (Rigaku) powder diffractometer in semifocusing (Bragg-Brentano) geometry using CuK$\alpha$ radiation ($\lambda$ = 1.54051 Å for CuK$\alpha_1$, and 1.54433 Å for CuK$\alpha_2$) in the 2$\theta$ range of 5—50 ° using a step size of 0.02 °; the diffracted beam was detected by one-dimensional semiconductor detector D/teX Ultra. Preliminary data processing was performed using the PDXL2 Rigaku software package (Rigaku corp., 2010), and the simulated powder diffraction pattern was calculated using the program *Mercury* (Macrae, 2020).

***X-ray Crystallography***
Single-crystal X-ray diffraction analysis of complexes **1—4** was done with a RIGAKU XtaLAB Synergy-S diffractometer equipped with CuK$\alpha$ radiation ($\lambda$ = 1.54184 Å, micro-focus X-ray source). The diffractometer was equipped with a Hybrid Pixel Area Detector (HyPix-6000HE). All data were collected at 100(2) K with the help of an Oxford Cryosystems (Cryostream 800) cooling device. CrysAlisPro software (Rigaku OD, 2023) was used for data collection, cell refinement, data reduction, and empirical absorption correction. Absorption effects were determined using the SCALE3 ABSPACK scaling algorithm and numerical absorption correction based on gaussian integration over a multifaceted crystal model (Coppens, 1965). The studied structures were solved with SHELXT-2018/2 (Sheldrick, 2015a) and refined using the program SHELXL-2018/3 (Sheldrick, 2015b). The structure of **2** exhibits strong pseudo-translational symmetry (0,1/2,0) due to the arrangement of heavy (Ni) atoms along the *b* axis. Anisotropic displacement parameters were refined for all non-H atoms. Hydrogen atoms bonded to carbon atoms were placed at idealized positions ($U_H$ = 1.2 $U_{eq}$ value of the corresponding parent atom). Positional parameters of hydrogen atoms bonded to the hetero N atoms were freely refined with a thermal parameter tied to the thermal parameter of the parent atom. Most hydrogen atoms in water molecules could be retrieved from the difference map and refined with restrained geometry ($U_H$ = 1.5 $U_{eq}$ value of the corresponding oxygen atom). Crystal data along with final parameters of the structure refinement for structures **1—4** are summarized in Tab. 1. Selected geometric parameters of **1—4** are shown in Tables 2, 3 and 5. Potential hydrogen bonds for structures **2** and **3** are gathered in Tables 4 and 6. Molecular graphics for all crystal

**Tab. 1.** Crystal data and structure refinement for **1**–**4**.

| | **1** | **2** | **3** | **4** |
|---|---|---|---|---|
| Empirical formula | $C_{19}H_{33}N_{12}O_8Ni$ | $C_{22}H_{32}N_{12}O_5Ni$ | $C_{18}H_{24}N_{14}NiO_6$ | $C_{18}H_{24}N_{12}F_6NiSi$ |
| Molecular weight | 616.28 | 603.30 | 591.22 | 609.29 |
| Crystal system | Hexagonal | Triclinic | Trigonal | Trigonal |
| Space group | $P6_3/m$ | $P$-1 | $R$-3 | $R$-3 |
| Cell parameters | | | | |
| $a$ (Å) | 8.9434(2) | 8.3434(2) | 12.3066(3) | 13.1803(3) |
| $b$ (Å) | 8.9434(2) | 9.8266(2) | 12.3066(3) | 13.1803(3) |
| $c$ (Å) | 20.8702(4) | 17.4587(3) | 14.4452(4) | 12.4447(3) |
| $\alpha$ (°) | 90 | 88.1410(10) | 90 | 90 |
| $\beta$ (°) | 90 | 81.640(2) | 90 | 90 |
| $\gamma$ (°) | 120 | 86.095(2) | 120 | 120 |
| $V$ (Å$^3$) | 1445.65(7) | 1412.52(5) | 1894.65(11) | 1872.26(10) |
| $Z$ | 2 | 2 | 3 | 3 |
| $D_{calc}$ (Mg · m$^{-3}$) | 1.416 | 1.418 | 1.554 | 1.621 |
| Abs. coeff. (mm$^{-1}$) | 1.521 | 1.466 | 1.685 | 2.312 |
| Crystal color, form | violet blue rhombohedra | purple prism | violet prism | violet prism |
| Crystal size (mm) | 0.177 × 0.133 × 0.108 | 0.188 × 0.140 × 0.073 | 0.252 × 0.112 × 0.093 | 0.280 × 0.210 × 0.140 |
| $T$ (K) | 100(2) | 100(2) | 100(2) | 100(2) |
| Radiation $\lambda$ (Å) | 1.54184 | 1.54184 | 1.54184 | 1.54184 |
| $\theta$ range (°) | 4.237–69.955 | 2.559–69.988 | 5.157–67.387 | 5.258–79.882 |
| Index ranges | $-10 \le h \le 10$ | $-8 \le h \le 10$ | $-14 \le h \le 14$ | $-16 \le h \le 16$ |
| | $-10 \le k \le 9$ | $-11 \le k \le 11$ | $-14 \le k \le 14$ | $-11 \le k \le 15$ |
| | $-25 \le l \le 21$ | $-21 \le l \le 21$ | $-17 \le l \le 17$ | $-13 \le l \le 15$ |
| Refl. coll./indep. | 4442/944 | 26329/5292 | 10512/765 | 3193/896 |
| Goodness-of-fit ($F^2$) | 1.124 | 1.093 | 1.096 | 1.101 |
| Final $R$ indices | $R1$ = 0.0357 | $R1$ = 0.0286 | $R1$ = 0.0240 | $R1$ = 0.0313 |
| ($I > 2\sigma(I)$) | w$R2$ = 0.0930 | w$R2$ = 0.0784 | w$R2$ = 0.0579 | w$R2$ = 0.0837 |
| $R$ indices (all data) | $R1$ = 0.0370 | $R1$ = 0.0307 | $R1$ = 0.0242 | $R1$ = 0.0324 |
| | w$R2$ = 0.0941 | w$R2$ = 0.0795 | w$R2$ = 0.0588 | w$R2$ = 0.0847 |
| Diff. peak and hole (e · Å$^{-3}$) | –0.517, 0.449 | –0.340, 0.236 | –0.281, 0.224 | –0.430, 0.259 |

structures were prepared using the DIAMOND program (Brandenburg, 2020).

## Results and Discussion

***Preparation and identification***

Among the four prepared complexes, $[Ni(H\mathit{im})_6]CO_3 \cdot 5H_2O$ (**1**), $[Ni(H\mathit{im})_6](\mathit{ac})_2 \cdot H_2O$ (**2**, *ac* = acetate), $[Ni(H\mathit{im})_6](NO_3)_2$ (**3**), and $[Ni(H\mathit{im})_6]SiF_6$ (**4**), complexes **2** and **4** are new, while crystal structures of **1** and **3** have already been reported in literature (Povse, 1998; Gong, 2005). Diffraction data for the already reported complexes **1** and **3** were collected on the same diffractometer under the same experimental conditions for better comparability. Interestingly, formation of the carbonate complex was unintentional as the carbonate anion was formed by the capture of $CO_2$ from air. Such a phenomenon is not uncommon; it was already observed. e.g. in $Zn_2(\mathit{tn})_2(CO_3)Ni(CN)_4 \cdot H_2O$ (*tn* = 1,3-diaminopropane) (Černák, 2005), $[Ni_2(\mathit{neoc})_4(H_2O)(CO_3)](NO_3)_2 \cdot 3H_2O$ (*neoc* = 2,9-dimethyl-1,10-phenanthroline) (Smolko, 2024), or the series of Schiff base Ni(II)/Ln(III) compounds: $\{(\mu_3\text{-}CO_3)_2[Ni(H\mathit{L})(EtOH)Ln(\mathit{ac})]_2\} \cdot 2EtOH$ (Ln(III) = Tb, Dy, Ho, Er, Tm, Yb) ($H_3L$ = N, N'-bis(3-methoxysalicylidene)-1,3-diamino-2-propanol; *ac* = acetate) (Jiang, 2017). Synthesis of the bulk compound **3** was carried out from Ni(II) nitrate hexahydrate, imidazole, and diammonium hexafluorosilicate in an acetone-ethanolic solution (1:1). The bulk as well as single crystals were identified using powder diffraction. For powder diffraction patterns fitting, the Le Bail method (Le Bail et al., 1988; Le Bail, 2005) incorporated in the Jana2006 program (Petříček, 2014) was used. The prepared complexes were characterized by CHN

analysis and IR spectroscopy. Characteristic absorption bands observed for both compounds were assigned using literature data (Nakamoto, 2009; Horák, 1976).

Measured IR spectrum of compound **1** corresponds to the previously reported $[Ni(H\mathit{im})_6]CO_3 \cdot 5H_2O$ (Povse, 1998); the sharp absorption band at 3643 $cm^{-1}$ was assigned to $\nu$(OH) stretching vibrations. The presence of H*im* in **1** is indicated by absorption bands in the region of 3129–3014 $cm^{-1}$ assigned to $\nu$(NH) stretching vibrations. The $\nu(C_{ar}—H)$ stretching vibrations manifest themselves by absorption bands in the region of 2919–2831 $cm^{-1}$. The corresponding deformation vibrations of $\delta(NH_2)$ and $\delta(CH_2)$ types lay within the range of 1686–1455 $cm^{-1}$. According to literature data, the carbonate anion is characterized by an absorption band arising from $\nu(CO_3^{2-})$ vibration positioned around 1390 $cm^{-1}$ (Povse, 1998). IR spectrum of **1** displays one strong absorption band at 1067 $cm^{-1}$, the corresponding band in $[Ni(H\mathit{im})_6]CO_3 \cdot 5H_2O$ (refcode SAXNEK) (Povse, 1998) is rather close (1071 $cm^{-1}$).

IR spectrum of **2** exhibits a wide absorption band at 3506 $cm^{-1}$ which was assigned to O—H stretching vibrations in $H_2O$. Absorption bands in the region of 3129–3025 $cm^{-1}$ were assigned to N—H stretching vibrations of H*im*. The C—H stretching vibrations manifest as an absorption band in the region of 2923–2834 $cm^{-1}$. Asymmetric $\nu_{as}$(COO) and symmetric $\nu_s$(COO) stretching vibrations of the acetate group were observed at 1571 $cm^{-1}$ and 1411 $cm^{-1}$, respectively. The experimental value of $\Delta$ = 160 $cm^{-1}$corresponds well to its ionic character (as predicted, $\Delta$ ionic is approximately 160–70 $cm^{-1}$ for acetates) (Nakamoto, 2009). IR spectrum of **3** is similar to the previously described $[Ni(H\mathit{im})_6](NO_3)$ (IMAZNI02) (Gong, 2005). A characteristic strong sharp absorption band originating from $\nu$(C—N) stretching vibrations was found at 1537 $cm^{-1}$.

In the IR spectrum of **4**, absorption bands from 3288 to 3141 $cm^{-1}$ indicating the presence of H*im* were assigned to the vibrations of the $\nu$(NH) group. Valence vibrations of the aromatic ring $\nu(C_{ar}—H)$ were observed in the region from 2945 to 2836 $cm^{-1}$. Deformation vibrations $\delta$(NH) were found at 1623 $cm^{-1}$. The strong absorption band at 1532 $cm^{-1}$ originates from the valence vibrations of the $\nu$(C—N) group. Valence vibrations $\nu$(C—C) originating from the aromatic ring H*im* were observed at 1432 $cm^{-1}$. According to available literature, absorption bands in the wavenumber range of 1100–600 $cm^{-1}$ are characteristic of the hexafluorosilicate anion $\nu$(Si—F) (Nakamoto, 2009), which were found at 795–693 $cm^{-1}$ in complex **4**.

### *Crystal structures*

Crystal structures of **1** (Wu, 2011) and **3** (Wu, 2011) have already been reported and the results of our structure analyses are essentially the same; both complexes **1** and **3** contain $[Ni(H\mathit{im})_6]^{2+}$ complex cations (Fig. 3 and 2) and the respective anions; in **1** there are additional water solvate molecules. The obtained geometric parameters correspond well to the reported ones. Selected geometric parameters are gathered in Tab. 2.

Ionic complex $[Ni(H\mathit{im})_6](\mathit{ac})_2 \cdot H_2O$ (**2**) (Fig. 3) is new and its crystal structure is formed by a $[Ni(H\mathit{im})_6]^{2+}$ complex cation, two acetate anions, and one solvate water molecule. In the unit cell, there are two crystallographically independent complex cations, in both of which the central atoms Ni1 and Ni2 lie at the centers of symmetry. Six H*im* ligands are monodentately bound to both

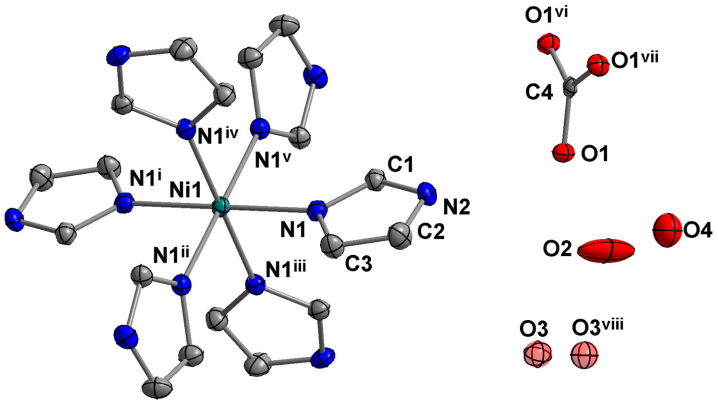


**Fig. 1.** Ionic structure of **1**. Thermal ellipsoids were drawn at 50 % probability level. Hydrogen atoms are omitted for clarity. Disordered O3 and $O3^{viii}$ atoms with half occupancies induced by symmetry are shown with transparency. Symmetry codes: i: *–x*, *–y*, 1 – *z*; ii: *x* – *y*, *x*, 1 – *z*; iii: *y*, *–x* + *y*, 1 – *z*; iv: *–y*, *x* – *y*, *z*; v: *–x* + *y*, *–x*, *z*; vi: *x*, *y*, 3/2 – *z*; vii: 2 – *y*, 1 + *x* – *y*, *z*; viii: 1 – *x* + *y*, 2 – *x*, *z*.

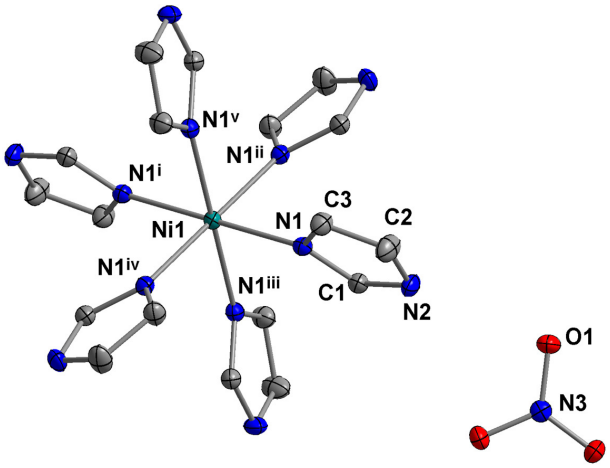


**Fig. 2.** Ionic structure of complex **3**. Thermal ellipsoids were drawn at 50 % probability level. Hydrogen atoms are omitted for clarity. Symmetry codes: i: 4/3 – *x*, 2/3 – *y*, 5/3 – *z*; ii: 1/3 + *y*, 2/3 – *x* + *y*, 5/3 – *z*; iii: 1/3 + *x* – *y*, –1/3 + *x*, 5/3 – *z*; iv: 1 – *y*, *x* – *y*, *z*; v: 1 – *x* + *y*, 1 – *x*, *z*; vi: –*x* + *y*, 1 – *x*, *z*; vii: 1 – *y*, 1 + *x* – *y*, *z*.

Ni(II) central atoms via the nitrogen atom in position 3. The $NiN_6$ chromophores represent slightly deformed octahedra, and the Ni—N distances are in the range of 2.1067(11)–2.1269(11) Å (Tab. 4). Packing of the crystal structure of **2** is governed, in addition to Coulombic forces, by O—H···O and N—H···O hydrogen bonds between $[Ni(Him)_6]^{2+}$ complex cations and solvate water molecules. Possible hydrogen bonds are provided in Tab. 4.

Crystal structure of $[Ni(Him)_6]SiF_6$ (**4**) is built up of complex cation $[Ni(Him)_6]^{2+}$ and hexafluorosilicate anion $(SiF_6)^{2-}$. Six *Him* ligands are monodentately bonded to the central Ni(II) atom through the nitrogen atom in position 3. The chromophore is $NiN_6$, with an almost ideal octahedral coordination polyhedron (Fig. 4). Bond distances for selected atoms are listed in Tab. 5; Ni—N distance is 2.1199(12) Å, N—C distances in aromatic imidazole ligands range from 1.323(2) Å to 1.379(2) Å, and Si—F distances in the hexafluorosilicate anion are 1.6917(8) Å. Values of the N—Ni—N and F—Si—F angles close to the right angle indicate an almost regular octahedral arrangement in both the complex cation and the hexafluorosilicate anion.

**Tab. 2.** Selected geometric parameters (Å, °) in 1 and **3**, comparison with literature data.

| Bond/angle | 1 | SAXNEK01 | 3 | IMAZNI03 |
|---|---|---|---|---|
| Ni—N | 2.1220(14) | 2.1173(15) | 2.1190(11) | 2.1152(11) |
| N1—Ni1—N1$^{ii}$ | 89.80(5) | 89.77(6) | 88.11(4) | 88.11(4) |
| N1$^{i}$—Ni1—N1$^{ii}$ | 90.20(5) | 90.23(6) | 91.90(4) | 91.89(4) |

Symmetry codes for **1**: i: –*x*, –*y*, 1 – *z*; ii: *x* – *y*, *x*, 1 – *z*.

Symmetry codes for **3**: i: 4/3 – *x*, 2/3 – *y*, 5/3 – *z*; ii: 1/3 + *y*, 2/3 – *x* + *y*, 5/3 – *z*.

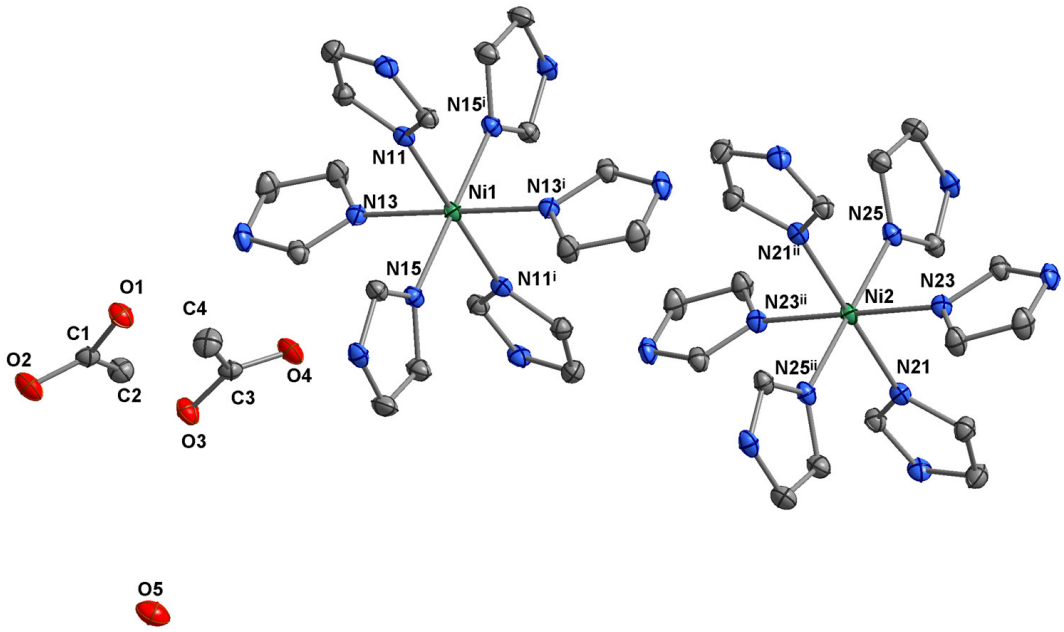


**Fig. 3.** Ionic structure of complex **2**. Thermal ellipsoids were drawn at 50 % probability level. Hydrogen atoms are omitted for clarity. Symmetry codes: i: –*x*, 1 – *y*, 1 – *z*; ii: –*x*, 1 – *y*, –*z*.

**Tab. 3.** Selected geometric parameters (Å, °) in **2**.

| | | | |
|---|---|---|---|
| Ni1—N11 | 2.1092(10) | N11—Ni1—N13 | 89.26(4) |
| Ni1—N13 | 2.1242(10) | N11—Ni1—N15 | 90.11(4) |
| Ni1—N15 | 2.1237(10) | N11i—Ni1—N13 | 90.74(4) |
| Ni2—N21 | 2.1067(11) | N21—Ni2—N23 | 89.78(4) |
| Ni2—N23 | 2.1178(10) | N21—Ni2—N25 | 89.59(4) |
| Ni2—N25 | 2.1269(11) | N21ii—Ni2—N23 | 90.22(4) |

Symmetry codes: i: –*x*, –*y* + 1, –*z* + 1; ii: –*x*, *y* + 1, –*z*.

**Tab. 4.** Possible hydrogen bonds in **2** (Å, °).

| D—H···A | D—H | H···A | D···A | D—H···A |
|---|---|---|---|---|
| O5—H1O5···O4$^{iv}$ | 0.85 | 2.00 | 2.8154(15) | 160.1 |
| O5—H2O5···O2$^{v}$ | 0.87 | 2.03 | 2.8970(15) | 170.8 |
| N12—H12N···O3$^{iii}$ | 0.84 | 1.89 | 2.7359(15) | 171.3 |
| N14—H14N···O1 | 0.79 | 1.99 | 2.7707(15) | 163.0 |
| N16—H16N···O4 | 0.84 | 1.86 | 2.6979(15) | 167.9 |
| N22—H22N···O1$^{vi}$ | 0.83 | 1.89 | 2.7169(15) | 169.1 |
| N24—H24N···O3$^{vii}$ | 0.81 | 1.92 | 2.7198(15) | 165.9 |
| N26—H26N···O2$^{vii}$ | 0.83 | 1.84 | 2.6661(15) | 171.2 |

Symmetry codes: iii: *x* + 1, *y*, *z*; iv: *x*, *y* + 1, *z*; v: *x* – 1, *y*, *z*; vi: *x*, *y*, *z* – 1; vii: *x* – 1, *y*, *z* – 1.

**Tab. 5.** Selected geometric parameters (Å, °) in **4**.

| | | | |
|---|---|---|---|
| Ni1—N1 | 2.1199(12) | N1$^{i}$—Ni1—N1$^{ii}$ | 89.19(5) |
| Si1—F1 | 1.6917(8) | N1$^{ii}$—Ni1—N1 | 90.81(5) |

Symmetry codes: i: 1/3 + *x* – *y*, –1/3 + *x*, 2/3 – *z*; ii: 1 – *y*, *x* – *y*, *z*.

**Tab. 6.** Possible hydrogen bonds in **4** (Å, °).

| D—H···A | D—H | H···A | D···A | D—H···A |
|---|---|---|---|---|
| N2—H2N···F1$^{ix}$ | 0.88 | 2.21 | 2.9378(16) | 140.4 |
| N2—H2N···F1$^{x}$ | 0.88 | 2.03 | 2.8266(16) | 150.6 |

Symmetry codes: ix: 5/3 – *x*, 4/3 – *y*, 4/3 – *z*; x: 4/3 – *x* + *y*, 5/3 – *x*, –1/3 + *z*.

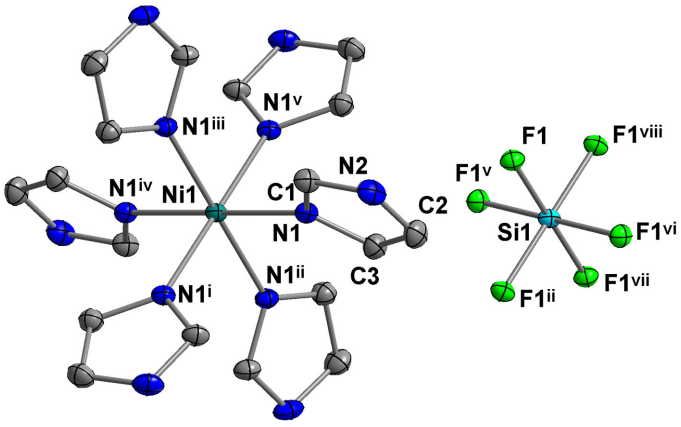


**Fig. 4.** Ionic structure of complex **4**. Thermal ellipsoids were drawn at 50 % probability level. Hydrogen atoms are omitted for clarity. Symmetry codes: i: 1/3 + *x* – *y*, –1/3 + *x*, 2/3 – *z*; ii: 1 – *y*, *x* – *y*, *z*; iii: 1/3 + *y*, 2/3 – *x* + *y*, 2/3 – *z*; iv: 4/3 – *x*, 2/3 – *y*, 2/3 – *z*; v: 1 – *x* + *y*, 1 – *x*, *z*; vi: 1/3 + *x* – *y*, –1/3 + *x*, 5/3 – *z*; vii: 4/3 – *x*, 2/3 – *y*, 5/3 – *z*; viii: 1/3 + *y*, 2/3 – *x* + *y*, 5/3 – *z*.

In the crystal structure of complex **4**, a system of intermolecular hydrogen bonds of the N—H···F type was observed between the complex cation $[Ni(Him)_6]^{2+}$ and the hexafluorosilicate anion. Possible hydrogen bonds are summarized in Tab. 6.

### *Comparison of the structures of $[Ni(Him)_6]^{2+}$ complex cations*

The search in CSD (Groom, 2016) returned more than 60 hits for compounds comprising $[Ni(Him)_6]^{2+}$ complex cations. For further comparison, only high precision crystal structures were used, i.e. those with reported *R*1 values below 5 % (38 complexes). For further detailed comparison of selected geometric parameters associated with the $NiN_6$ chromophore, only those were considered for which the X-ray data were gathered at low temperature (up to 120 K); there are only eight structures (six compounds) fulfilling these criteria including the four reported in this work (REF codes of already reported structures are in bold) (Tab. 7). In these compounds, the counter-anions are two perchlorate anions in $[Ni(Him)_6](ClO_4)_2$ (Wu, 2011), two nitrate anions in $[Ni(Him)_6](NO_3)_2$ (Wu, 2011), a biphenyldicarboxylate anion in $[Ni(Him)_6](bph(COO)_2)\cdot H_2O$ (Chand, 2019), and a carbonate anion in $[Ni(Him)_6]CO_3\cdot 5H_2O$ (Wu, 2011). For detailed comparison of $NiN_6$ chromophores, see Tab. 8; where the Ni—N distances are shown along with the calculated values of the OC-6 parameter from the SHAPE program (Llunel, 2013) indicating the deviation of the $NiN_6$ chromophores from a regular octahedron. As it can be seen, the $[Ni(Him)_6]^{2+}$ cations display an almost ideal octahedral shape in all studied complexes. The highest deviations, according to the SHAPE program, were observed in $[Ni(Him)_6](bph(COO)_2)\cdot H_2O$ (Chand, 2019) and in complex **3**. Differences in the shapes of the respective polyhedra in different complexes were visualized through overlays of the respective pairs of complex cations using the Mercury program. Selected examples are shown in Fig. 5, showing significant differences in the orientation of H*im* rings in the respective compounds. Consequently, angles between the $NiN_4$ plane and the plane through the H*im* ligand (more precisely through the C and N atoms) — the tilting angles, were determined (Tab. 8). Differences in the tilting angles can be ascribed to the action of intermolecular forces, more precisely the formation of hydrogen bonds; the H*im* ligand takes an orientation that maximizes the possibility of forming intermolecular interactions and minimizes the repulsion within the coordination sphere.

**Tab. 7.** Structures containing $[Ni(Him)_6]^{2+}$ with various anions measured at low temperature.

| REF code | Formula | R1 factor | Reference |
|---|---|---|---|
| **HIMZNJ02** | $[Ni(Him)_6](ClO_4)_2$ | 4.50 | Wu, 2011 |
| **IMAZNI03** | $[Ni(Him)_6](NO_3)_2$ | 2.58 | Wu, 2011 |
| **MIVQOA** | $[Ni(Him)_6](bph(COO)_2)\cdot H_2O$ | 4.48 | Chand, 2019 |
| **SAXNEK01** | $[Ni(Him)_6]CO_3\cdot 5H_2O$ | 4.14 | Wu, 2011 |
| **1** | $[Ni(Him)_6]CO_3\cdot 5H_2O$ | 3.70 | This work |
| **2** | $[Ni(Him)_6](ac)_2\cdot H_2O$ | 3.07 | This work |
| **3** | $[Ni(Him)_6](NO_3)_2$ | 2.42 | This work |
| **4** | $[Ni(Him)_6]SiF_6$ | 3.24 | This work |

**Tab. 8.** Selected complexes with $[Ni(Him)_6]^{2+}$ cation with geometric parameters characterizing the $NiN_6$ chromophore.

| REF code | Formula | Ni—N [Å] | OC-6 Shape | Tilting angle [°] | Reference |
|---|---|---|---|---|---|
| **HIMZNJ02** | $[Ni(Him)_6](ClO_4)_2$ | 2.129(2) | 0.031 | 6.68, 12.08, 21.96 | Wu, 2011 |
| **IMAZNI03** | $[Ni(Him)_6](NO_3)_2$ | 2.1152(11) | 0.029 | 22.99 | Wu, 2011 |
| **3** | $[Ni(Him)_6](NO_3)_2$ | 2.1190(11) | 0.056 | 23.24 | This work |
| **MIVQOA** | $[Ni(Him)_6](bph(COO)_2)\cdot H_2O$ | 2.1409(18) | 0.056 | 4.58, 10.64, 16.48 | Chand, 2019 |
| **SAXNEK01** | $[Ni(Him)_6]CO_3\cdot 5H_2O$ | 2.1174(15) | 0.001 | 8.83 | Wu, 2011 |
| **1** | $[Ni(Him)_6]CO_3\cdot 5H_2O$ | 2.1220(14) | 0.001 | 8.92 | This work |
| **2** | $[Ni(Him)_6](ac)_2\cdot H_2O$ | 2.1269(11) | 0.004 | 3.42, 4.44, 4.82, 7.76, 8.40, 16.76 | This work |
| **4** | $[Ni(Him)_6]SiF_6$ | 2.1199(12) | 0.010 | 13.48 | This work |

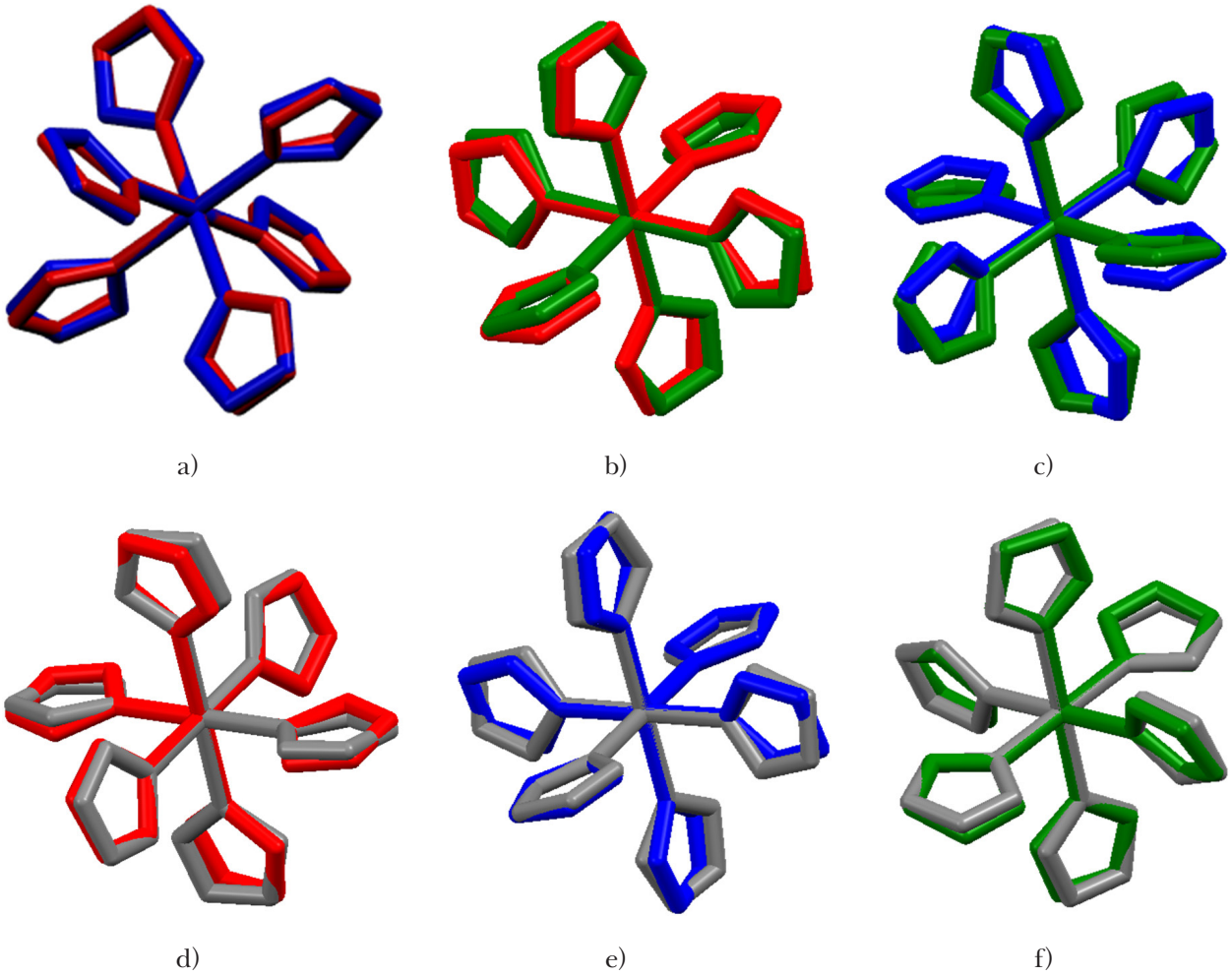


**Fig. 5.** Comparisons of molecular structures of the respective complex cations containing Ni1 central atom. The complex cations were superimposed in such a way that the $NiN_6$ chromophores were put as close to each other as possible. a) **1** (red) and **2** (blue), b) **1** (red) and **3** (green), c) **2** (blue) and **3** (green), d) **1** (red) and **4** (grey), e) **2** (blue) and **4** (grey), f) **3** (green) and **4** (grey).

## Conclusions

Four Ni(II) complexes containing $[Ni(H\mathit{im})_6]^{2+}$ (H*im* = imidazole) were prepared. Two complexes have previously been described in literature: $[Ni(H\mathit{im})_6](CO_3)\cdot 5H_2O$ (**1**), and $[Ni(H\mathit{im})_6](NO_3)_2$ (**3**), while $[Ni(H\mathit{im})_6](\mathit{ac})_2\cdot H_2O$ (**2**, *ac* = acetate) and $[Ni(H\mathit{im})_6]SiF_6$ (**4**) are new. Complex **1** was prepared unintentionally, by capturing $CO_2$ from air into the structure. Results of single crystal studies have shown that all four complexes exhibit ionic crystal structures built up of $[Ni(H\mathit{im})_6]^{2+}$ complex cations, the respective anion(s) and in case of **1** and **2**, additional solvate water molecules. While in **1** and **4,** the $NiN_6$ chromophores are quite regular octahedra with only one independent Ni—N bond; in **2** and **3,** the octahedra are slightly deformed. On the other hand, some differences in the orientation of H*im* rings within the coordination polyhedra were observed; these were ascribed to the action of intermolecular forces.

*Acknowledgments*

*We thank Dr. M. Litecká from the Institute of Inorganic Chemistry of the Czech Academy of Sciences, for X-ray single crystal data collections.*

*Funded by the EU NextGenerationEU through the Recovery and Resilience Plan for Slovakia under the project No. 09I03-03-V05-00008.*

## Supplementary data

Crystallographic data for compounds **1**–**4** are deposited in the Cambridge Crystallographic Data Centre, CCDC no. 2504734 (**4**), 2504735 (**2**), 2504736 (**1**), 2504737 (**3**), respectively. The data can be obtained free of charge via http://www.ccdc.cam.ac.uk/conts/retrieving.html, or from the Cambridge Crystallographic Data Centre, 12 Union Road, Cambridge CB2 1EZ, UK; fax: (+44) 1223-336-033; or e-mail: deposit@ccdc.cam.ac.uk.

## References


Brandenburg K, Putz H (2020) Program DIAMOND (Version v4.6.3). Crystal Impact GbR, Bonn, Germany.

Brezovan M, Juráková J, Moncoľ J, Dlháň Ľ, Korabik M, Šalitroš I, Pavlik J, Segľa P (2022) Inorganics 10(9): 128.

Coppens P, Leiserowitz L, Rabinovich D (1965) Acta Crystallogr., 18: 1035—1038.

Černák J, Ferencová B, Žák Z (2005) Polyhedron, 24: 579—584.

Černák J, Farkašová N, Tomás M, Kavečanský V, Čižmár E, Orendáč M (2015) J. Coord. Chem. 68(16): 2788—2797.

Ding Y, Gao DS, Li SD, Li XH, Li CL (2009) Koord. Khim. (Russ. Coord. Chem). 35: 663—667.

Gong Y, Hu Ch, Li H, Pan W, Niu X, Pu Z (2005) J. Mol. Struct. 740: 153—158.

Groom CR, Bruno IJ, Lightfoot MP, Ward SC (2016) Acta Crystallogr. B72: 171—179.

Horák M, Papoušek D (1976) Infračervená spectra a struktura molekul. Academia, Praha. ISBN 509-21-857.

Chand S, Chand Pal S, Pal A, Ye Y, Lin Q, Zhang Z, Xiang S, Das MC (2019) Chem.-Eur. J. 25: 1691.

Ivaniková R, Boča R, Dlháň L, Fuess H, Mašlejová A, Mrázová V, Svoboda I, Titiš J (2006) Polyhedron 25: 3261—3268.

Jiang L, Liu Y, Liu X, Tian J, Yan S (2017) Dalton Trans. 46: 12558—12573.

Juráková J, Midlíková J, Hrubý J, Kliuikov A, Santana VT, Pavlik J, Moncoľ J, Čižmár E, Orlita M, Mohelský I, Neugebauer P, Gentili D, Cavallini M, Šalitroš I (2022) Inorg. Chem. Front. 9: 1179—1194.

Joshi S, Chowdhury SR, Mishra S (2025) Cryst. Growth Des. 25(8): 2602—2616.

Le Bail A, Duroy H, Fourquet JL (1988) Mater. Res. Bull. 23: 447—452.

Le Bail A (2005) Powder diffr. 20(4), 316—326.

Llunell M, Casanova D, Cirera J, Alemany P, Alvarez S (2013) SHAPE Program, version 2.1, Universitat de Barcelona.

Krešáková L, Miňo A, Holub M, Kuchár J, Werner A, Tomás M, Čižmár E, Falvello LR, Černák J (2021) Inorg. Chim. Acta 527: 120588.

Leiszner SS, Perfetti M, Damgaard-Møller E, Chen YS, Iversen BB (2024) Dalton Trans. 53(48): 19246—19255.

Manson JL, Manson ZE, Sargent A, Villa DY, Etten NL, Blackmore WJA, Curley SPM, Williams RC, Brambleby J, Goddard PA, Ozarowski A, Wilson MN, Huddart BM, Lancaster T, Johnson RD, Blundell SJ, Bendix J, Wheeler KA, Lapidus SH, Xiao F, Birnbaum S, Singleton J (2020) Polyhedron 180: 114379.

Macrae CF, Sovago I, Cottrell SJ, Galek PTA, Mccabe P, Pidcock E, Platings M, Shields GP, Stevens JS, Towler M, Wood PA (2020) Mercury 4.0: from visualization to analysis, design and prediction. J. Appl. Cryst. 53: 226—235.

Mašlejová A, Ivaniková R, Svoboda I, Papánková B, Dlháň L, Mikloš D, Fuess H, Boča R (2006) Polyhedron 25: 1823—1830.

Nakamoto K (2009) Infrared and Raman Spectra of Inorganic and Coordination Compound, 6th Edition, J. Wiley & Sons, New York.

Petříček V, Dušek M, Palatinus L (2014) Z. Kristallogr., 229: 345—352.

Povse V, Perec M, Baggio R, Garland MT (1998) Acta Crystallogr. C54: 1817—1820.

Rigaku OD (2023). CrysAlisPro. Retrieved from https://rigaku.com/products/crystallography/x-ray-diffraction/crysalispro

Sheldrick GM (2015b) Acta Crystallogr. C71: 3.

Sheldrick GM (2015a) SHELXT — Integrated space-group and crystal-structure determination, Acta Crystallogr. A71: 3—8.

Singh SK, Gupta T, Badkur P, Rajaraman G (2014) Chem. Eur. J. 20: 10305—10313.

Smolko R, Dušek M, Kuchár J, Čižmár E, Černák J (2024) Polyhedron 255: 116953.

Song JF, Zhou RS, Xu XY, Liu YB, Wang TG, Xu JQ (2008) J. Mol. Struct. 874 (1-3): 34—40.

Šterbinská S, Holub M, Kuchár J, Čižmár E, Černák J (2020) Polyhedron 187: 114654.

Titiš J, Boča R (2010) Inorg. Chem. 49: 3971—3973.

Vráblová A, Falvello LR, Campo J, Miklovič J, Boča R, Černák J, Tomás M (2016) Eur. J. Inorg. Chem. 928—934.

Wu BD, Wang SW, Yang L, Zhang TL, Zhang JG, Zhou ZN (2011) Z. Anorg. Allg. Chem. 637: 2252—2259.